Blocking M1 repolarization of M2 THP-1 macrophages through inhibition of the type I interferon response by vesicular stomatitis virus

by

Melissa Marie Rowe

Honors Thesis

Appalachian State University

Submitted to the Department of Biology

and The Honors College

in partial fulfillment of the requirements for the degree of

Bachelor of Science

May 2021

Approved by:

Darren Seals, Ph.D., Thesis Director

Megen Culpepper, Ph.D., Second Reader

Lynn Siefferman, Departmental Honors Director

Jefford Vahlbusch, Ph.D., Dean, The Honors College

Abstract

Matrix protein mutant strains of VSV, such as rM51R-M virus, are currently being investigated as oncolytic agents due to their ability to target and kill cancer cells while also stimulating innate immunity. We seek to examine the ability of rM51R-M virus to modulate tumor promoting M2 macrophages as a means to inhibit the progression of cancer. In the tumor microenvironment, M2 macrophage activity has a suppressive effect on the immune system, which can lead to tolerance of tumor cells. M1 macrophages, in contrast, stimulate an immune response and reduce tumor cell viability. Our lab has previously shown that rM51R-M virus re-educates M2 macrophages to an M1-like phenotype, but the mechanism by which it does so remains unknown. In THP-1 polarized M2 macrophages, we have observed increased levels of IFNα, total STAT1, and p-STAT1 upon infection with rM5IR-M virus. We hypothesize that the ability of rM51R-M virus to stimulate the type I IFN antiviral pathway in M2 macrophages may coerce them to an M1-like phenotype. To test this hypothesis, we seek to examine the effects of the p-STAT1 inhibitor fludarabine on macrophage polarization by rM51R-M virus. M2 macrophages were pretreated with different concentrations of fludarabine (50, 100, or 150 μM), infected with rM51R-M virus (MOI 1 or 10 pfu/cell) for 24 hours, and subjected to immunoblot analysis for total and phosphorylated STAT1. Results indicated that when cells were infected with rM51R-M virus at an MOI of 1, STAT1 phosphorylation was reduced to between 23% (50 μM fludarabine) and 16 % (100 and 150 μM fludarabine) of control levels. Similar results were obtained when cells were infected at an MOI of 10. These results confirm that fludarabine is capable of inhibiting the accumulation of p-STAT1. Therefore, this reagent can be used to reduce type I IFN signaling

in order to determine the extent to which this pathway modulates macrophage identity during rM51R-M infection. Such mechanistic insights will be important in understanding the multipotent effects of VSV as an oncolytic agent.

Acknowledgements

I would like to thank Dr. Darren Seals for his insight, support, and patience through seemingly endless drafts of this thesis. He has been a true mentor to me throughout my time at Appalachian and I would not be the person or scientist I am today without him. I would also like to thank Dr. Maryam Ahmed for her guidance and expertise throughout the many steps of this project. I want to thank Dr. Megen Culpepper for her willingness to be on my thesis committee despite the crazy year we've all had. To Sylas Owen, Brewer Logan, Gabrianne Ivey, Emma Wandscher, and so many other members of the Seals and Ahmed labs, past and present, thank you for growing with me, laughing with me, and sharing your passion and knowledge of biology with me. Finally, thank you to Appalachian State University, the Department of Biology, the Honors College, and the Garrett family for providing the funding and resources that made this project possible.

Table of Contents

List of Abbreviations

BCA: bicinchoninic acid

BHK: baby hamster kidney

BSA: bovine serum albumin

CAR-T cells: chimeric antigen receptor T-cells

CCL: chemokine (C-C motif) ligand

CD: cluster of differentiation (often used as an identity marker)

CSF1: colony stimulating factor 1

DMSO: dimethyl sulfoxide

EGF: epidermal growth factor

HLA-DR: human leukocyte antigen-DR isotype

IFNI: interferon type I (includes interferon alpha, beta, and others)

IFNAR: human type I interferon receptor

IL: interleukin

iNOS: inducible isoform of nitric oxide synthase

IRF: interferon regulatory factor

JAK1: Janus kinase 1

M1: inflammatory macrophage

M2: immunosuppressive macrophage

MDA-MB-231: human triple-negative breast cancer cell line

MMP: matrix metalloproteinase

MOI: multiplicity of (viral) infection

MyD88: adaptor protein in the TLR signaling pathway leading to NFκB activation

NCI: National Cancer Institute

NFκB: nuclear factor kappa-light-chain-enhancer of activated B cells

Nos2: nitric oxide synthase 2

PBS: phosphate buffered saline

PD-L1: programmed death-ligand 1

pfu: plaque forming units

PMA: phorbol 12-myristate 13-acetate

p-STAT1: phosphorylated signal transducer and activator of transcription 1

RIPA buffer: radioimmunoprecipitation assay buffer

rM51R-M virus: matrix protein mutant of vesicular stomatitis virus (change of methionine to arginine at position 51)

SDS: sodium dodecyl sulfate

TAM: tumor associated macrophage

TBS-T: Tris-buffered saline containing Tween 20

TGF-β: transforming growth factor beta

THP-1: human monocytic leukemia cell line

TLR: toll-like receptor

TNF-α: tumor necrosis factor alpha

Tris: tris(hydroxymethyl)aminomethane

VEGF: vascular endothelial growth factor

VSV: vesicular stomatitis virus

Introduction

According to the National Cancer Institute (NCI), approximately 1 in 3 men and women will receive a cancer diagnosis in their lifetimes (Siegel et. al. 2019). Accordingly, the NCI has an annual budget exceeding $5 billion dollars. That money, along with resources from pharmaceutical companies and non-profits, supports a staggering infrastructure designed to alleviate the significant health and financial burdens caused by this disease. Yet despite this long-term effort that symbolically began with the National Cancer Act of 1971, standard-of-care treatments still rely on techniques developed decades ago, including surgery, radiation, and chemotherapy. These treatments often come with devastating side effects and are less effective at later stages of the disease when cancer cells have metastasized to distant regions of the body. Current research efforts seek to alleviate these issues with next generation cancer therapies. One proposed category of treatment is the recruitment of the patient's own immune system to fight against the tumor. In this vein, our project seeks to modulate the functionality of an immune cell, the macrophage, through the use of an oncolytic virus.

Macrophages are a component of the innate and adaptive immune systems. As blood monocytes with origins in the bone marrow, they specialize as they move into tissue in response to signaling molecules. Some macrophages are tissue-specific, such as the alveolar macrophages of the lungs or the microglia of the central nervous system. However, in most of the body's tissues, macrophages polarize based on the needs of the immune system at the time of monocyte maturity.

Macrophages were previously classified using a binary system that separated them into M1 or M2 phenotypes (Locati et. al. 2020). However, additional research has shown that macrophages are more heterogeneous than formerly believed, with phenotypes that parallel the diverse signals that activate them (Xue et. al. 2014, Roussel et. al. 2017). For example, IL-4 and IL-10 polarize macrophages to the M2 phenotype. However, macrophages stimulated with only IL-4 or only IL-10 exhibited significant phenotypic differences from each other, suggesting that it may be beneficial to categorize them separately (Roussel et. al. 2017). Still, the M1 and M2 distinction can be useful for defining macrophages based on their more general functions. M1 macrophages, for example, are pro-inflammatory and promote T-cell activity. These macrophages also assist in the clearance of pathogenic bacteria and have antitumoral properties. Human M1 macrophages express HLA-DR, iNOS, CD86, and p-STAT1 in higher proportion than their M2 counterparts. They also secrete inflammatory cytokines like IL-6, IL-12, IL-23, and TNF-α, as well as reactive oxygen and nitrogen species (Jayasingam et. al. 2020, Locati et. al. 2020). M2 macrophages, in contrast, express higher levels of CD206, CD204, CCL22, CCL17, and CD163 and secrete cytokines that suppress immune activity like IL-10, PD-L1, and TGF-β. They also exert tissue repair functions by secreting adrenomedullin and VEGF, both of which support the growth of blood vessels (Jayasingam et. al. 2020, Locati et. al. 2020). The immunosuppressive nature of M2 macrophages helps diminish over-stimulation of the immune system and promotes normal tissue growth (Petty and Yang 2017). Ultimately it is the balance between M1 and M2 macrophage phenotypes that allows the body to protect itself from harmful pathogens while also preventing and repairing damage to its own tissues.

Macrophage populations within the tumor microenvironment have long been implicated in the development of aggressive cancers. A 2017 meta-analysis of breast cancer patient data revealed that a high density of tumor-associated macrophages (TAMs) resulted in increased markers of aggressive cancer and correlated with lower overall survival (Zhao et. al. 2017). This is largely attributable to a high density of M2 macrophages in the tumor microenvironment. M2 macrophages make up such a large proportion of TAMs that the terms are sometimes used interchangeably. The prevalence of this subtype among TAMs is due to cytokines secreted by tumor cells that promote M2 polarization, such as CSF1 and TGF-β (Petty and Yang 2017). In the context of cancer, the M2 subtype is detrimental to the patient, causing the immune system to tolerate the presence of the tumor. M2 macrophages also directly promote cancer cell growth, angiogenesis, and metastasis. These pro-tumor functions occur as a result of cytokine and surface signaling on M2 macrophages, including but not limited to VEGF, which promotes angiogenesis, EGF, which is a pro-tumoral growth factor, and MMPs, a class of proteases that aid in tissue remodeling during cancer cell invasion and metastasis (Anfray et. al. 2019, Zhao et. al. 2017, Petty and Yang 2017).

Not all TAMs are pro-tumoral. The M1 subtype among TAM populations can be beneficial to the patient. They promote the activation of cytotoxic T-cells and generate reactive nitrogen and oxygen species that contribute to cancer cell death. M1 TAMs have shown promise for the clearance of melanoma in mouse models of the disease (Petty and Yang 2017). The pro-inflammatory, anti-tumor properties of M1 macrophages make them desirable in a patient's tumor microenvironment.

Modulation of macrophage identity is a promising avenue for anti-cancer therapies. Some common therapeutic strategies of macrophage modulation include inhibition of

macrophage movement to the tumor site and the conversion of M2 TAMs into M1 TAMs. Suppression or depletion of all TAMs (or just M2 TAMs) are also popular strategies (Tariq et. al. 2017). Each strategy shows promise and can employ multiple therapeutic techniques. For example, CAR-T cells are one possible avenue of M2 macrophage depletion. Chimeric antigen receptor (CAR)-T cells are modified leukocytes containing a genetically engineered CAR protein that identifies a selected target antigen. They are typically used to destroy cancer cells expressing disease-specific proteins (Sermer and Brentjens, 2019). CAR-T cells have also been used to target and eliminate TAMs expressing M2 markers. An ovarian cancer mouse model displayed slower tumor growth and increased survival when such macrophage depletion was coupled with tumor-targeting CAR-T cells as opposed to tumor targeting alone (Rodriguez-Garcia et. al. 2021). Another research group found that the chemotherapeutic agent hydroxychloroquine suppresses non-small cell lung cancer in part because it promotes the transition of M2 macrophages into an M1-like phenotype (Li et. al. 2018). These two examples represent just a fraction of the potential routes for clinically relevant macrophage alteration.

Another potential route for macrophage modulation is the use of oncolytic viruses. An oncolytic virus is one that can kill cancer cells with minimal damage to normal host tissue. These viruses can be either naturally occurring or genetically modified (Fukuhara et. al. 2016). My efforts have focused on vesicular stomatitis virus (VSV). VSV is a pathogen of livestock, such as horses and pigs, and is transmitted through an insect vector. Human infections are rare and mild, having mostly occurred in lab personnel working with the virus or in animal handlers. Multiple tissue culture cell lines are permissible to infection by wild-type VSV, making it particularly useful in both viral research and clinical applications. VSV

is capable of inducing apoptosis in cancer cells through multiple, independent mechanisms (Bishnoi et. al. 2018). It has specifically been shown to lyse cells in hypoxic tumor microenvironments, and therefore may alleviate the tumor-promoting stress associated with increased resistance to radiation and chemotherapy. In this way, the virus may sensitize tumor cells to chemotherapy (Bishnoi et. al. 2018). In addition to VSV's direct effects on tumor cells, the virus has shown the ability to indirectly lower tumor viability. As VSV can infect the tumor vasculature, the virus may lead to decreased blood flow and increased immune cell infiltration of the tumor (Bishnoi et. al. 2018).

Multiple clinical trials are investigating the use of VSV mutants as cancer therapies, many of which are modified to express IFNβ (Table 1). The inclusion of the IFNβ gene has been shown to improve the safety of the virus without compromising its anti-cancer properties (Kurisetty et. al. 2014). Other engineered VSV strains may also increase the cancer-fighting activity of tumor-associated immune cells while maintaining a high level of patient safety. One example is rM5IR-M, a matrix protein mutant of VSV. A change from methionine to arginine at position 51 in the matrix protein sequence renders the virus incapable of inhibiting host immune gene expression (Figure 1). Typically, matrix protein-mediated repression of host gene expression prohibits anti-viral responses in infected organisms. For example, most wild type VSV viruses suppress the type I IFN anti-viral response in the host, thus supporting continued viral infection. rM51R-M virus, however, upregulates this pathway, and thereby increases the immune modulatory capabilities of the virus, thus making rM51R-M an ideal oncolytic virus with which to enact phenotypic shifts in macrophage polarization (Ahmed et al. 2006). rM51R-M virus has also shown low replicative potential in normal tissue, increasing its safety in patients (Ahmed et al. 2006).

Table 1. ***VSV variants currently in clinical trials.***

VSV Variant	Cancer(s) Targeted	Trial #	Phase
Voyager V1 (IFNβ mutant)	Melanoma Hepatocellular Carcinoma Non Small Cell Lung Cancer Endometrial Cancer	NCT04291105	2
Recombinant VSV expressing IFNβ	Advanced Malignant Solid Neoplasm Hepatocellular Carcinoma	NCT01628640	1
VSV-IFNβ-NIS	Malignant Solid Tumor	NCT02923466	1
VSV-IFNβ-NIS	Solid Tumor Head and Neck Squamous Cell Carcinoma Non Small Cell Lung Cancer	NCT03647163	1

Information was obtained via ClinicalTrials.gov.

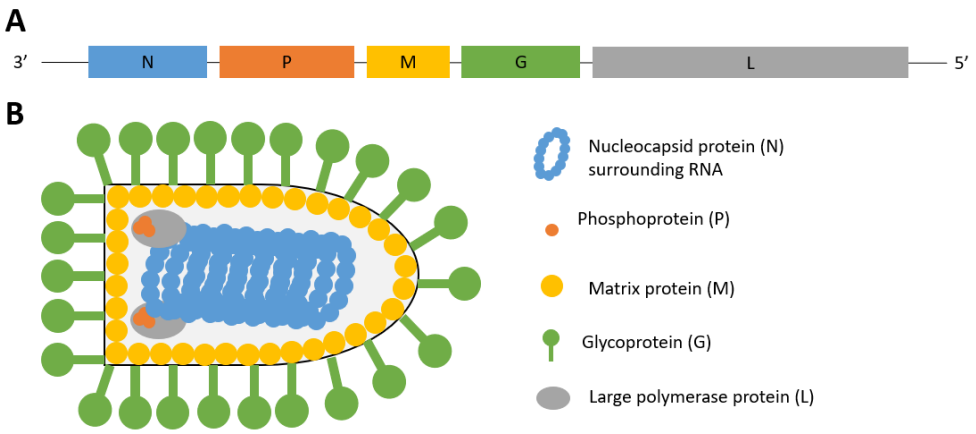

Figure 1. ***Genomic and morphological structure of wild type VSV.*** *Panel A shows the orientation of genes along the negative-stranded RNA genome of VSV. Panel B shows the protein localization within a single viral particle. Images are based on those from the Swiss Institute of Bioinformatics and Michael Dumiak.*

Previous experiments in our lab have shown that rM5IR-M virus may polarize macrophages towards a more inflammatory phenotype. This is indicated by the increased expression of the M1 markers p-STAT1, CD80, and TNF-α following infection of a M2 THP-1 macrophage population (Polzin 2020). Additionally, in a co-culture of M2 THP-1 macrophages and MDA-MB-231 breast cancer cells, infection with rM51R-M virus resulted in a significant reduction of the M2 marker IL-10 (McCanless 2019). Therefore, macrophages appear to be moving away from the immunosuppressive M2 subtype as a result of rM51R-M viral infection.

Like many viruses, rM51R-M virus stimulates the type I interferon (IFN) pathway. This pathway participates in anti-viral responses as well as M1 macrophage polarization

(Figure 2). Viral infection stimulates the production of type I IFNs (IFNα or IFN β) in most cell types (Samuel 2001). When IFNα or IFN β binds to the IFNα/β receptor (IFNAR), it stimulates the autophosphorylation of JAK1. This triggers the phosphorylation of STAT1, which forms a dimer with phosphorylated STAT2. The dimer then associates with IRF9 and moves into the nucleus where it induces an antiviral response (Figure 2A) (Ivashkiv and Donlin 2014). This response includes the production of proteins that damage or prevent translation of viral RNA, as well as proteins targeting viral nucleocapsids. IFN signaling can also lead to the production of major histocompatibility antigens, which recruit cytotoxic T cells, and nitric oxide synthase, which can produce reactive chemical species that kill viruses (Samuel 2001). Transcriptional regulation by this pathway also leads to the production of additional IFNα/β.

The type I IFN pathway can also take part in M1 macrophage polarization. The STAT1/2 dimer produced by the type I IFN pathway (typically as a result of IFNβ signaling) can synergize with NFκB downstream of toll-like receptor (TLR) activation. This synergy leads to transcriptional regulation of, for example, Nos2, a gene producing some of the reactive nitrogen species characteristic of M1 macrophages (Figure 2B) (Müller et. al. 2018). The type I IFNs that trigger M1 polarization may come from virus-infected cells. They may also come from previously activated macrophages or dendritic cells (another immune cell population). Other M1 markers are upregulated by this signaling pathway as well.

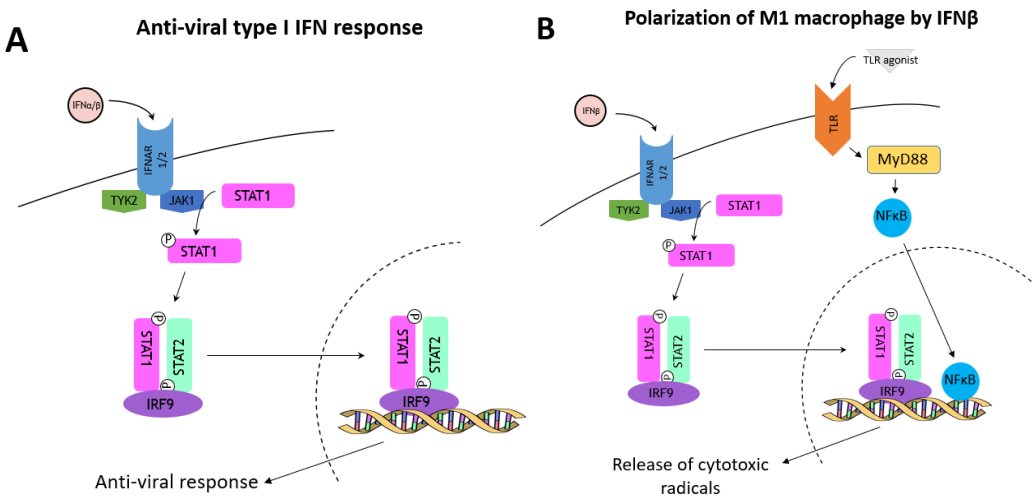

Figure 2. ***Comparison of type I IFN pathways during an antiviral response and during M1 macrophage polarization.*** *Panel A shows the type I IFN pathway that leads to an anti-viral response. Following the binding of a type I IFN to IFNAR, JAK1 phosphorylates STAT1, which forms a dimer with phosphorylated STAT2. The dimer then associates with IRF9 and moves into the nucleus to modulate transcription, leading to upregulation of anti-viral proteins. Panel B shows the polarization of an M1 macrophage by IFNβ. The pathway is very similar to the anti-viral response, with a phosphorylated STAT1-STAT2 dimer associating with IRF9 before moving into the nucleus. However, in M1 macrophages, this complex synergizes with NFκB to alter transcription, leading to the release of reactive nitrogen species. NFκB comes from a signaling pathway activated by a TLR binding to its ligand. Multiple ligand-TLR pairs can activate this pathway. MyD88 acts as an adapter protein, passing the signal from the receptors to NFκB. Images are based on those found in Owen (2020) and Müller et. al. (2018).*

The rM51R-M strain of VSV has been shown to upregulate components of the type I IFN pathway in M2 THP-1 macrophages. The increase in total and phosphorylated STAT1 over samples infected with wild-type VSV was previously mentioned (Polzin 2020). There is also an increase in IFNα signal propagation in rM51R-M virus-infected macrophages (Owen 2020). It has been further established that VSV is extremely sensitive to the type I IFN family of molecules (Bishnoi et. al. 2018). Therefore, we hypothesize that rM51R-M virus modulates macrophages to a more inflammatory phenotype via the type I IFN pathway.

In order to determine the role of the type I IFN pathway in macrophage repolarization, we have attempted to chemically inhibit STAT1 phosphorylation/activation with fludarabine. Fludarabine is a chemical analog of the antiviral agent vidarabine and a known inhibitor of STAT1 phosphorylation (Figure 3). The mechanism of action by which fludarabine inhibits the accumulation of p-STAT1 is not well characterized. STAT1 has two phosphorylation sites, Y710 and S727. A 2014 study of fludarabine activity in melanoma samples indicated downregulation of phosphorylation at both sites (Hanafi et. al. 2014). However, as the S727 site becomes phosphorylated downstream of the Y710 site, it is unclear if fludarabine directly targets the S727 site or if less phosphorylation occurs due to upstream downregulation of Y710. Fludarabine is also a chemotherapeutic agent marketed under the name Fludara®. It exhibits a cytotoxic effect on B-cell malignancies such as B-cell chronic lymphocytic leukemia and mantle cell lymphoma (Baran-Marszak et. al. 2004). In addition, ^{18}F-fludarabine, a radioactive conjugate of fludarabine, has been used in lymphoma imaging, as it is specifically taken up by cells with high glucose metabolism (Barré et. al. 2019). Therefore, it is an important substance to study in the context of cancer treatment because it can be taken up so readily and has several clinical applications.

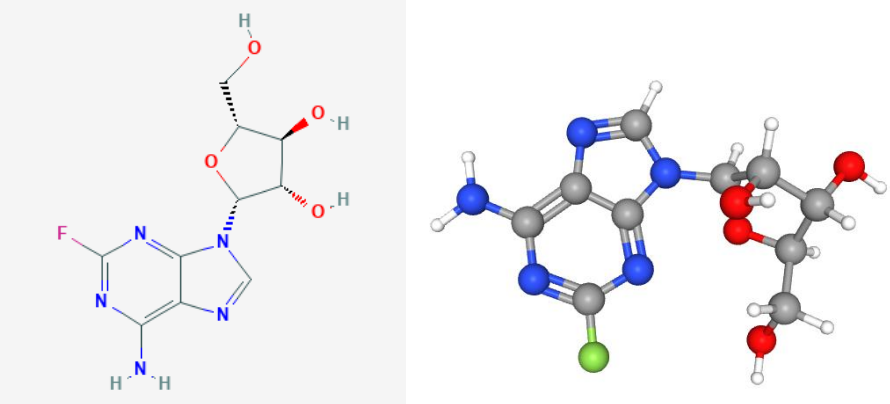

Figure 3. ***2D and 3D models of fludarabine.*** *Images retrieved from PubChem.*

Our research uses THP-1 cells as a model of human macrophages. THP-1 is an immortalized human monocytic leukemia cell line that can be matured and polarized into a variety of macrophage phenotypes. PMA can be used to differentiate THP-1 monocytes into adherent macrophages (Chanput et. al. 2014). Subsequent treatment with the cytokines IL-4 and IL-13 polarizes these THP-1 macrophages to an M2 phenotype (Locati et. al. 2020). In the experiments presented here, THP-1 monocytes were pre-polarized to an M2 phenotype before treating the cells with fludarabine and infecting with rM51R-M virus (Figure 4). While the virus can repolarize these M2 macrophages to a more M1-like profile, it was expected that the fludarabine-treated M2 macrophages would retain their phenotype following viral infection. However, prior to an exhaustive characterization of macrophage marker expression, the concentration of fludarabine capable of inhibiting the phosphorylation of STAT1 under these assay conditions had to be determined. Therefore, a titration experiment was performed to determine the minimum concentration of fludarabine at which p-STAT1 accumulation would be inhibited to levels comparable to uninfected and untreated

M2 THP-1 macrophage populations. This minimum concentration would then be selected for future experimentation.

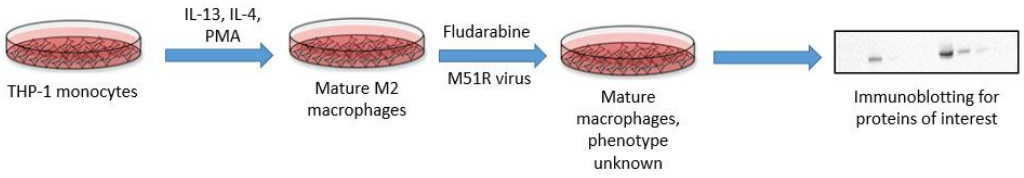

Figure 4. ***Experimental workflow.*** *THP-1 monocytes were matured and polarized to M2 macrophages using PMA, IL-4, and IL-13, exposed to fludarabine, and then infected with rM51R-M virus. Cell lysates were then collected and proteins detected and quantified by immunoblotting.*

Methods and Materials

Cells and Virus

THP-1 monocytic leukemia cells were propagated in RPMI media (Corning, 10-040-CV) supplemented with 10% fetal bovine serum (R&D Systems, S11150) and 0.05 mM 2-mercaptoethanol (MP Biomedicals, 190242) between 2 x 10^5 and 1 x 10^6 cells/ml. The rM51R-M strain of VSV was a gift from Dr. Douglas Lyles of the Wake Forest University School of Medicine (Winston-Salem, NC) and has been previously described (Whitlow et al. 2006). Viral stocks were grown in BHK fibroblasts for 24 hours, spun down, and collected into cryovials, then stored at -80°C (Kopecky et al., 2001). Virus was thawed on ice, then added to M2-polarized THP-1 macrophages at a MOI of 1 or 10 pfu/cell for a 24-hour infection period.

M2 Macrophage Polarization

THP-1 cells were transferred to a 6-well plate at a concentration of 1.4 x 10^6 cells/well. Here they were subsequently polarized to an adherent, M2 macrophage phenotype through a step-wise 24-hour incubation in THP-1 media containing 25nM PMA followed by a 48-hour incubation in THP-1 media containing 25nM PMA, 20ng/mL IL-4, and 20ng/mL IL-13. Stocks of PMA (Sigma-Aldrich, P1585) were made as 25μM solutions in DMSO. Stocks of IL-4 (Bio-Legend, 574002) and IL-13 (Bio-Legend, 571102) were made as 20μg/mL

solutions in 0.05% BSA/PBS. All stock solutions were kept at -80˚C in small volume aliquots that at most were thawed and refrozen 1-3 times.

Fludarabine Treatment

Pre-polarized M2 macrophages were treated with fludarabine (Selleckchem, S1491) at 50, 100, or 150 μM for 1 hour prior to infection with rM51R-M virus for 24 hours as described above. Fludarabine was diluted directly in THP-1 media.

Cell Lysis

Following experimental manipulations, the cells were washed twice with ice-cold PBS before being scraped into 100 μl of ice-cold RIPA buffer. The RIPA buffer consisted of 50 mM Tris-HCl (pH 8.0), 150mM NaCl, 1.0% NP-40, 0.5% sodium deoxycholate, 0.1% SDS, and 1 μg/mL aprotinin (Fisher Scientific, ICN19455910). The samples were centrifuged at 16,000x*g* for 20 min, the pellets discarded, and the supernatants analyzed for protein content using a Pierce™ BCA Protein Assay Kit (Thermo Scientific, 23225) according to manufacturer's instructions against a series of BSA standards. Cell lysates were incubated at 95°C with an equal volume of 2X Laemmli sample buffer for 5 minutes before storing at -80°C.

Immunoblotting

For immunoblot analysis, 20µg of lysate protein was loaded onto a 10% polyacrylamide gel, separated by SDS-PAGE, and then transferred to a 0.45µm nitrocellulose membrane (Bio-Rad, 1620115) at 100V for 1 hour. After blocking in 5% milk/TBS-T for 1 hour, membranes were washed 3 times at 5 minutes each in TBS-T. Membranes were then incubated overnight at 4°C with primary antibody to p-STAT1 (Y701) (Cell Signaling, 9167S) at 1:1000 in 5% BSA/TBS-T. Membranes were washed as previously described before incubation with a peroxidase-conjugated secondary antibody (GE Healthcare, NA9340V) at 1:2000 in 5% dry milk/TBS-T for 1 hour at room temperature. Proteins were visualized using SuperSignal™ West Dura Extended Duration Substrate (ThermoFisher Scientific, 34075) or SuperSignal™ West Pico PLUS Chemiluminescent Substrate (ThermoFisher Scientific, 34080) and Image Lab software (Bio-Rad). Image Lab was used to perform the densitometry analysis. This was done from the pixels in a 19 mm^2 area centered over the darkest region for each band.

Results

The rM51M-R strain of VSV upregulates the M1 macrophage markers p-STAT1, CD80, and TNF-α in a pre-polarized M2 macrophage population (Polzin 2020). The virus also reduces secretion of IL-10, a cytokine associated with M2 macrophages (McCanless 2019). It is suspected that this virus is shifting the macrophages towards a tumor-fighting M1 phenotype, but the mechanism is not fully appreciated. There are similarities between the antiviral type I IFN pathway and the signaling pathways involved in M1 polarization (Figure 2). Both increase the phosphorylation-dependent activation of the transcription factor STAT1. Fludarabine is a small molecule inhibitor of STAT1 phosphorylation/activation. Here it was hypothesized that fludarabine would block the repolarization of M2 macrophages if the type I IFN pathway was responsible for this phenomenon. This experiment sought to determine a fludarabine concentration capable of inhibiting STAT1 phosphorylation under the assay conditions being employed.

M2 polarized THP-1 macrophages were pre-treated with fludarabine, then infected with rM51R-M virus at an MOI of 1 or 10 pfu/cell for 24 hours, after which lysates were analyzed for the expression of p-STAT1 (see Figure 4). Mock-infected M2 macrophages were also examined as a negative control. Mock-infected M2 THP-1 macrophages exhibited low levels of p-STAT1 (Figure 5A). While the band was not visible to the naked eye, densitometry analysis returned some p-STAT1 signal, which is likely caused by background noise (Figure 5B). This was in contrast to those macrophages subjected to infection with the rM51R-M virus, which displayed increases in p-STAT1 levels (Figure 5). These data

therefore reaffirm former studies that have shown an increase in STAT1 phosphorylation following infection with the mutant virus (Polzin 2020).

The effect of fludarabine on p-STAT1 levels was as hypothesized with reductions in STAT1 phosphorylation (Figure 5A). At an MOI of 1 pfu/cell, STAT1 phosphorylation was reduced to between 23% (50 μM fludarabine) and 16 % (100 and 150 μM fludarabine) of the levels present without the drug (Figure 5B). This was comparable to the results at an MOI of 10 pfu/cell, which reduced the levels of p-STAT1 to 32% (50 μM fludarabine) or 16% (100 μM fludarabine) of the levels present without the drug (Figure 5B). Fludarabine at a concentration of 150μM reduced STAT1 phosphorylation to a level comparable to background signaling (Figure 5).

As well as effectively inhibiting p-STAT1, none of the concentrations tested had a noticeable effect on the viability of THP-1 cells. Cells were visualized prior to lysate collection, and there were no notable signs of cell death, such as floating cells and lower plate density. In addition, a protein assay performed on a similar experiment yielded no large differences in total protein concentration between rM51R-M-infected THP-1 cells treated with fludarabine and those not treated with fludarabine. In this experiment, lysates from fludarabine-treated samples had total protein concentrations between 606.4 μg/mL and 665.1 μg/mL. Lysates from samples with no fludarabine had total protein concentrations between 624.7 μg/mL and 719.7 μg/mL. Although the total protein concentration is lower in the fludarabine-treated samples, there was not enough of a difference to discourage use of fludarabine at this concentration. Collectively, these data indicate that 100μM fludarabine may be sufficient for future studies where STAT1 inhibition will be tested for its ability to block the repolarization of M2 macrophages.

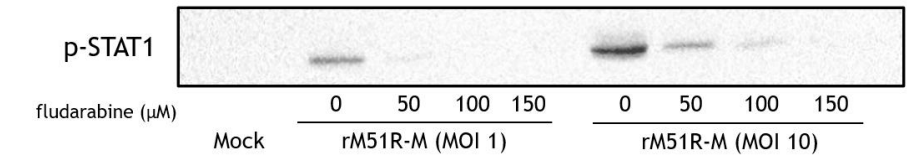

A

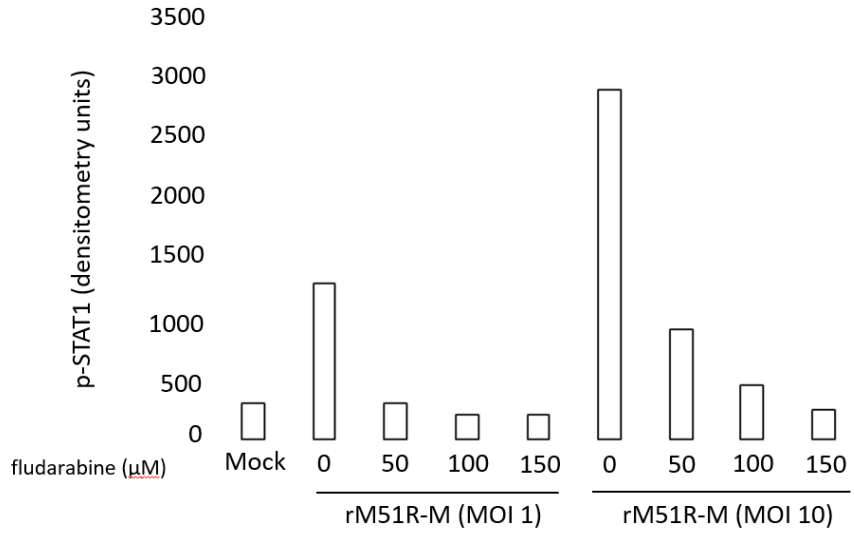

B

Figure 5. ***Fludarabine inhibits p-STAT1 accumulation in M2 THP-1 macrophages following infection with rM51R-M virus.*** *Panel A: THP-1 monocytes were pre-differentiated into macrophages and polarized to an M2 phenotype. Cells were then treated with fludarabine at 0, 50, 100, or 150 μM for one hour prior to a 24-hour infection with rM51R-M virus (MOI of 1 or 10 pfu/cell) (see Figure 4). Mock indicates no drug treatment and no virus infection. Total cell lysates were subjected to immunoblot analysis by probing with a p-STAT1 antibody. Panel B: The immunoblot data in Figure 5A was subjected to densitometry analysis in order to quantitate proteins levels of phosphorylated STAT1.*

Discussion

Previous experiments in our lab have shown that a mutant strain of the oncolytic vesicular stomatitis virus, rM51R-M, can reduce M2 markers and activate M1-polarizing STAT1 signaling in a THP-1 macrophage population (Polzin 2020). The overarching goal of this project was to determine the effects of p-STAT1 inhibition on this re-education of M2 macrophages. To that end, fludarabine at a concentration ranging from 50 to 150 μM was tested for inhibition of STAT1 phosphorylation. Effectiveness of inhibition was determined by comparison to M2-polarized macrophages that were not subjected to inhibition with fludarabine or infection with rM51R-M. Fludarabine exhibited inhibition of STAT1 phosphorylation at all concentrations tested, indicating that this inhibitor is active under the conditions of our assay.

This experiment used MOIs of 1 and 10 to represent both asynchronous and synchronous infections with rM51R-M virus. An MOI of 1 pfu/cell resembles a natural infection where the virus will infect and replicate in some cells before spreading to others. This will evoke a systematic antiviral response meant to arrest the progression of a natural infection. An MOI of 10 pfu/cell models a synchronous infection, in which nearly every cell in a system is infected during the introduction of the virus. This allows for the study of the antiviral response of individual cells, as viral spread between cells will be limited (Owen 2020). The extent of the infection, natural (MOI of 1) or synchronous (MOI of 10), elicited increasing effects on STAT1 phosphorylation, which was over 2-fold higher under the higher viral load (Figure 5). Similarly, the extent of inhibition by fludarabine also depended on the multiplicity of infection—the more virus used in the assay, the more fludarabine was needed

for full inhibition. In a compromise between maximum effectiveness of the drug with presumed limited cytotoxicity, 100 μM is currently considered the ideal fludarabine concentration for further experimentation. Although 150 μM fludarabine exhibited slightly more inhibition of STAT1 phosphorylation, 100 μM was sufficient to bring levels of p-STAT1 down to a level comparable to uninfected M2 macrophages at both MOIs. Using this lower, but still effective, concentration of fludarabine will also allow for more efficient use of this resource.

STAT1 is not the only marker that can be used to validate the role of type I interferon signaling in the repolarization of M2 macrophages in response to VSV infection. Others include cell surface markers like HLA-DR, CD11c, and CD86 for M1 macrophages, and CD163, CD204, and CD206 for M2 macrophages. The presence of these markers can be determined by flow cytometry. This single-cell analytical method will more clearly indicate whether individual macrophages are fully or partially displaying macrophage identity markers, which cannot be seen in a measure of aggregate protein by immunoblot analysis. The molecules secreted by macrophages are also potential targets for macrophage identification. M1 macrophages secrete the pro-inflammatory cytokines IL-6, IL-12, and IL-23, while M2 macrophages secrete IL-10, PD-L1, and TGF-β (Jayasingam et. al. 2020). These molecules can be quantified using an ELISA assay. The markers of macrophage identity previously used in our lab include p-STAT1, CD204, IL-6, TNF-α, and IL-10. Therefore, these are the markers that will receive most of our attention to facilitate comparisons to previous work. Marker expression will be compared to that of untreated M1 or M2 macrophages to give an indication of the identity of macrophage populations exposed

to the virus and fludarabine. This step of the project is already in progress, as the initial experimental steps are completed up to the collection of cell lysates.

In addition to western blotting, ELISAs, and/or flow cytometry, functional assays will be used to characterize macrophages. A phagocytosis assay for THP-1 macrophages is currently in development in our lab. Preliminary data suggests that M2 THP-1 macrophages exhibit a ~10-fold higher phagocytic index than M1 THP-1 macrophages based on the uptake of fluorescently-labeled *E.coli* particles. Moreover, the rM51R-M mutant of VSV reduced phagocytosis in M2 macrophages by 50% (Simmons, Seals, and Ahmed, personal communications). Experiments to test fludarabine's impact on these results are being planned. As phagocytosis is a trademark behavior of macrophages, this assay will allow further differentiation of macrophage identity based on functional activity (Locati et. al. 2020).

The importance of such an extensive examination of macrophage markers/activity is due to the lack of full phenotype characterization of macrophages modulated by rM51R-M virus. Infection with rM51R-M virus has been shown to increase expression of the M1 markers p-STAT1, CD80, and TNF-α and reduce expression of the M2 marker IL-10 in M2 THP-1 macrophages (Polzin 2020, McCanless 2019). However, no change was observed in the M2 macrophage marker CD204 upon infection with rM5IR-M virus (Polzin 2020). Macrophages appear to be moving away from the immunosuppressive M2 subtype as a result of rM51R-M viral infection, but they do not completely shed canonical markers of this subtype. It is possible that infected macrophages assume an intermediate phenotype between M1 and M2. By performing a full characterization of macrophage markers in our samples,

we will be able to more accurately describe the population of macrophages emerging post-infection.

As there are multiple components in the type I IFN pathway, there are multiple ways to validate its role in the repolarization of M2 macrophages by rM51R-M virus. One such experiment might consist of IFNα and IFNβ inhibition. This will be done using a human type I interferon neutralizing antibody mixture (Fisher Scientific 50-153-8053 [PBL Assay Science]). The mixture includes antibodies directed against the human type I interferon receptor as well as several of its ligands, including IFNα and IFNβ themselves. We expect that this reagent will have similar downstream effects as fludarabine. Importantly, inhibiting another molecule in the IFNα/β pathway will either reaffirm the findings from the fludarabine experiment or indicate an alternative mode of macrophage repolarization if the results are not comparable.

If type I interferon signaling antagonists fail to block universal changes in macrophage phenotype or lead to intermediate phenotypes, then it could indicate that this pathway is not solely responsible for macrophage re-education as a result of rM51R-M viral infection. The reason for this would need additional research to determine. It could be that the type I IFN pathway does not play a role at all in macrophage identity shift. It is also possible that the type I IFN pathway plays a role, but that other pathways compensate for its loss when inhibition occurs. To this end, additional experiments will be performed with the purpose of determining the extent of activation in other pathways under our experimental conditions, such as activation of TLR and NFκB.

The TLR pathway is of interest for future experimentation. Wild-type VSV has been shown to stimulate a subset of dendritic cells through TLR7 and MyD88 (Ahmed et. al.

2009). However, stimulation of other dendritic cell subsets by rM51R-M virus occurred in a way that was largely independent of TLR7 and MyD88. Yet, rM51R-M virus upregulated NFκ-B in dendritic cells over mock-infected samples (Ahmed et. al. 2009). Although dendritic cells are an immune population distinct from macrophages, it is possible that rM51R-M virus has similar effects on the pathways these populations share. As such, it is possible that r-M51R-M virus creates synergy between STAT1/2 and NFκ-B signaling in macrophages through a pathway different than the one outlined in Figure 2. While beyond the scope of this study, the question of whether r-M51R-M virus activates the TLR/MyD88 pathway in macrophages is a possible avenue for further experimentation.

Our study is hardly the first one to examine the effects of oncolytic viruses on macrophage identity. Passaro found that the oncolytic adenovirus dl922-947 prevents the infiltration of M2 macrophages into anaplastic thyroid carcinoma tumors (Passaro et. al. 2016). It does this by reducing the production of CCL2 by cancer cells. *In vitro*, this reduction lowered monocyte chemotaxis. The virus also shifted macrophages towards an M1 phenotype *in vivo*, as seen by increased Nos2 expression (Passaro et. al. 2016). Another study showed that an oncolytic virus increased inflammatory macrophage activity (Tan et. al. 2016). Attenuated paramyxoviruses (the class of virus that measles and mumps belong to) were found to be more effective at breast cancer tumor clearance when virally-infected macrophages were present. This could be attributable to the increase in M1 macrophage markers seen in virus-infected samples. M1-associated tumoricidal mediators were also found to be responsible for reduced tumor viability *in vitro* (Tan et. al. 2016). When combined with the studies published by Polzin (2020) and extended as part of this thesis, it

seems clear that macrophage repolarization can be a novel therapeutic benefit of oncolytic virotherapies.

This research also has implications for the use of fludarabine in the clinic. As stated prior, fludarabine is administered as a chemotherapy under the name Fludara®, and is also utilized in cancer imaging. If fludarabine is found to inhibit the shift of macrophages to a phenotype more beneficial for the patient, it would raise questions about the use of fludarabine when patients are receiving an oncolytic virotherapy.

Here we have validated the use of fludarabine as an inhibitor of STAT1 signaling induced by infection of M2 THP-1 macrophages with a mutant strain of VSV called rM51R-M. Further research will substantiate the extent to which such signaling yields repolarization of macrophages to an anti-tumor M1 population, but if so, oncolytic viruses capable of re-training the immune system to clear cancerous cells could become another tool in oncology's therapeutic arsenal.

Works Cited

Ahmed M, Brzoza KL, and Hiltbold EM (2006). Matrix Protein Mutant of Vesicular Stomatitis Virus Stimulates Maturation of Myeloid Dendritic Cells. *Journal of Virology 80*(5): 2194-2205. doi: 10.1128/JVI.80.5.2194-2205.2006

Ahmed M, Mitchell LM, Puckett S, Brzoza-Lewis KL, Lyles DS, and Hiltbold EM (2009). Vesicular Stomatitis Virus M Protein Mutant Stimulates Maturation of Toll-like Receptor 7 (TLR7)-positive Dendritic Cells through TLR-dependent and -independent Mechanisms. *Journal of Virology*; 83(7), 2962–2975. https://doi.org/10.1128/JVI.02030-08

Anfray C, Ummarino A, Andón FT, and Allavena P (2019). Current Strategies to Target Tumor-Associated-Macrophages to Improve Anti-Tumor Immune Responses. *Cells*; 9(1):46. doi: 10.3390/cells9010046.

Baran-Marszak F, Feuillard J, Najjar I, Le Clorennec C, B chet JM, Dusanter-Fourt I, Bornkamm GW, Rapha l M, and Fagard R (2004). Differential Roles of STAT1α and STAT1β in Fludarabine-induced Cell Cycle Arrest and Apoptosis in Human B Cells. *Blood*; 104 (8): 2475–2483. doi: https://doi.org/10.1182/blood-2003-10-3508

Barré L, Hovhannisyan N, Bodet-Milin C, Kraeber-Bodéré F, and Damaj G (2019). [18F]-Fludarabine for Hematological Malignancies. *Frontiers in Medicine (Lausanne) 6*:77. doi: 10.3389/fmed.2019.00077

Bishnoi S, Tiwari R, Gupta S, Byrareddy SN, and Nayak D (2018). Oncotargeting by Vesicular Stomatitis Virus (VSV): Advances in Cancer Therapy. *Viruses*. 10(2):90. doi:10.3390/v10020090

Chanput W, Mes JJ, Wichers HJ (2014). THP-1 Cell Line: An in Vitro Cell Model for Immune Modulation Approach. *International Immunopharmacology*; 23(1):37-45. doi: 10.1016/j.intimp.2014.08.002.

Frank D, Mahajan S, and Ritz J (1999). Fludarabine-induced Immunosuppression is Associated with Inhibition of STAT1 Signaling. *Nature Medicine* 5, 444–447. https://doi.org/10.1038/7445

Fukuhara H, Ino Y, and Todo T (2016). Oncolytic Virus Therapy: A New Era of Cancer Treatment at Dawn. *Cancer Science* 107(10):1373-1379. doi: 10.1111/cas.13027.

Hanafi LA, Gauchat D, Godin-Ethier J, Possamaï D, Duvignaud JB, Leclerc D, Grandvaux N, & Lapointe R. (2014). Fludarabine downregulates indoleamine 2,3-dioxygenase in tumors via a proteasome-mediated degradation mechanism. *PloS one*, 9(6), e99211. https://doi.org/10.1371/journal.pone.0099211

Ivashkiv LB and Donlin LT (2014). Regulation of Type I Interferon Responses. *Nature reviews. Immunology*, *14*(1), 36–49. https://doi.org/10.1038/nri3581

Jayasingam SD, Citartan M, Thang TH, Zin AAM, Ang KC, and Ch'ng ES (2020). Evaluating the Polarization of Tumor-Associated Macrophages into M1 and M2 Phenotypes in Human Cancer Tissue: Technicalities and Challenges in Routine Clinical Practice. *Frontiers in Oncology (Radiation Oncology)*. https://doi.org/10.3389/fonc.2019.01512

Kopecky SA, Willingham MC, Lyles DS (2001). Matrix Protein and Another Viral Component Contribute to Induction of Apoptosis in Cells Infected with Vesicular Stomatitis Virus. *Journal of Virology*; 75(24):12169-81. doi: 10.1128/JVI.75.24.12169-12181.2001.

Kurisetty VV, Heiber J, Myers R, Pereira GS, Goodwin JW, Federspiel MJ., Russell SJ, Peng KW, Barber G, and Merchan, JR (2014). Preclinical Safety and Activity of Recombinant VSV-IFN-β in an Immunocompetent Model of Squamous Cell Carcinoma of the Head and Neck. *Head & neck*; 36(11), 1619–1627. https://doi.org/10.1002/hed.23502

Li Y, Cao F, Li M, Li P, Yu Y, Xiang L, Xu T, Lei J, Tai YY, Zhu J, Yang B, Jiang Y, Zhang X, Duo L, Chen P, and Yu X (2018). Hydroxychloroquine Induced Lung Cancer Suppression by Enhancing Chemo-sensitization and Promoting the Transition of M2-TAMs to M1-like Macrophages. *Journal of Experimental & Clinical Cancer Research.* 37(1):259. doi: 10.1186/s13046-018-0938-5.

Locati M, Curtale G, and Mantovani A (2020). Diversity, Mechanisms, and Significance of Macrophage Plasticity. *Annual Review of Pathology: Mechanisms of Disease*;15:123-147. doi:10.1146/annurev-pathmechdis-012418-012718

McCanless J (2019). Modulation of Breast Tumor Associated Macrophages by Oncolytic Vesicular Stomatitis Virus. *Master's Thesis available on NC DOCKS*. Appalachian State University, Boone, NC.

Müller E, Speth M, Christopoulos PF, Lunde A, Avdagic A, Øynebråten I, and Corthay A (2018). Both Type I and Type II Interferons Can Activate Antitumor M1 Macrophages When Combined with TLR Stimulation. *Frontiers in Immunology*; *9*, 2520. https://doi.org/10.3389/fimmu.2018.02520

Owen S (2020). The Type I Interferon Anti-Viral Pathway Contributes to Macrophage Polarization Following Infection with Oncolytic Vesicular Stomatitis Virus. *Master's Thesis available on NC DOCKS*. Appalachian State University. Boone, NC.

Passaro C, Borriello F, Vastolo V, Di Somma S, Scamardella E, Gigantino V, Franco R, Marone G, and Portella G (2016). The Oncolytic Virus dl922-947 Reduces IL-8/CXCL8 and MCP-1/CCL2 Expression and Impairs Angiogenesis and Macrophage Infiltration in Anaplastic Thyroid Carcinoma. *Oncotarget*, *7*(2), 1500–1515. https://doi.org/10.18632/oncotarget.6430

Petty AJ and Yang Y (2017). Tumor-associated Macrophages: Implications in Cancer Immunotherapy. *Immunotherapy*. 9(3):289-302. doi:10.2217/imt-2016-0135

Polzin M, McCanless J, Owen S, Sizemore D, Lucero E, Fuller R, Neufeld HS, Seals DF, Ahmed M (2020). Oncolytic vesicular stomatitis viruses selectively target M2 macrophages. *Virus Research*; 284:197991. doi: 10.1016/j.virusres.2020.197991.

Rodriguez-Garcia A, Lynn RC, Poussin M, Eiva MA, Shaw LC, O'Connor RS, Minutolo NG, Casado-Medrano V, Lopez G, Matsuyama T, and Powell DJ Jr (2021). CAR-T Cell-mediated Depletion of Immunosuppressive Tumor-associated Macrophages Promotes Endogenous Antitumor Immunity and Augments Adoptive Immunotherapy. *Nature Communications.* 12: 877. doi: 10.1038/s41467-021-20893-2

Roussel M, Ferrell PB Jr, Greenplate AR, Lhomme F, Gallou SL, Diggins KE, Johnson DB, and Irish JM (2017). Mass Cytometry Deep Phenotyping of Human Mononuclear Phagocytes and Myeloid-Derived Suppressor Cells from Human Blood and Bone Marrow. *Journal of Leukocyte Biology*. 102:437-447. doi: 10.1189/jlb.5MA1116-457R

Samuel CE (2001). Antiviral Actions of Interferons. *Clinical Microbiology Reviews*; 14(4), 778–809. https://doi.org/10.1128/CMR.14.4.778-809.2001

Sermer D and Brentjens R (2019). CAR T-cell Therapy: Full Speed Ahead. *Hematological Oncology*; 37 Suppl 1:95-100. doi: 10.1002/hon.2591.

Siegel RL, Miller KD. and Jemal A (2019). Cancer Statistics, 2019. *CA:A Cancer Journal for Clinicians*; 69: 7-34. https://doi.org/10.3322/caac.21551

Tan DQ, Zhang L, Ohba K, Ye M, Ichiyama K and Yamamoto N (2016). Macrophage Response to Oncolytic Paramyxoviruses Potentiates Virus-mediated Tumor Cell Killing. *European Journal of Immunology*; 46: 919-928. https://doi.org/10.1002/eji.201545915

Tariq M, Zhang J, Liang G, Ding L, He Q, and Yang B (2017). Macrophage Polarization: Anti-Cancer Strategies to Target Tumor-Associated Macrophage in Breast Cancer. *Journal of Cellular Biochemistry*; 118(9):2484-2501. doi: 10.1002/jcb.25895.

Whitlow ZW, Connor JH, Lyles DS (2006). Preferential Translation of Vesicular Stomatitis Virus mRNAs is Conferred by Transcription from the Viral Genome. *Journal of Virology*; 80(23):11733-42. doi: 10.1128/JVI.00971-06.

Xue J, Schmidt SV, Sander J, Draffehn A, Krebs W, Quester I, De Nardo D, Gohel TD, Emde M, Schmidleithner L, Ganesan H, Nino-Castro A, Mallmann MR, Labzin L, Theis H, Kraut M, Beyer M, Latz E, Freeman TC, Ulas T, and Schultze JL (2014). Transcriptome-based Network Analysis Reveals a Spectrum Model of Human Macrophage Activation. *Immunity*. 40(2):274-288. doi:10.1016/j.immuni.2014.01.006

Zhao X, Qu J, Sun Y, Wang J, Liu X, Wang F, Zhang H, Wang W, Ma X, Gao X, and Zhang S (2017). Prognostic Significance of Tumor-associated Macrophages in Breast Cancer: A Meta-analysis of the Literature. *Oncotarget*. 8(18):30576-30586. doi:10.18632/oncotarget.15736